Nanoscale

Accepted Manuscript

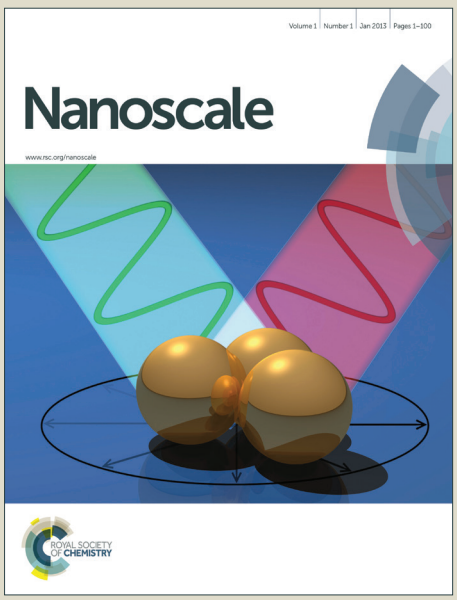

ROYAL SOCIETY OF CHEMISTRY

www.rsc.org/nanoscale

Nanoscale

RSCPublishing

ARTICLE

Investigation on the binding modes between AIE-active molecules and *ds*DNA by single molecule force spectroscopy

Cite this: DOI: 10.1039/x0xx00000x

Received 00th January 2015,
Accepted 00th January 2015

DOI: 10.1039/x0xx00000x

www.rsc.org/nanoscale

Ying Chen[‡a], Ke Ma[‡a], Ting Hu[b], Bo Jiang[a], Bin Xu[a], Wenjing Tian[a], Jing Zhi Sun[b], Wenke Zhang*[a]

AIE (aggregation-induced emission)-active molecules hold the promise for the labeling of biomolecules as well as living cells. The study of the binding modes of such molecule to biomolecules, such as nucleic acid and protein, will shed light on a deeper understanding of the mechanism of molecular interactions and eventually facilitate the designing/preparation of new AIE-active bioprobes. Here, we studied the binding modes of double-stranded DNA (*ds*DNA) with two types of synthetic AIE-active molecules, tetraphenylethene-derived dicationic compounds (*cis*-TPEDPy, *trans*-TPEDPy) and anthracene-derived dicationic compounds (DSAI, DSABr-C6), by using single molecule force spectroscopy (SMFS) and circular dichroism (CD) spectroscopy. The experimental data indicate that DSAI can intercalate into DNA base pairs strongly, while DSABr-C6 is unable to intercalate into DNA due to the steric hindrance of the alkyl side chains. *Cis*-TPEDPy and *trans*-TPEDPy can also intercalate into DNA base pairs, but the binding shows strong ionic strength dependence. Multiple binding modes of TPEDPy with *ds*DNA have been discussed. And the electrostatic interaction enhanced intercalation of *cis*-TPEDPy with *ds*DNA has also been revealed.

Introduction

Aggregation-induced emission (AIE) phenomenon was first reported in 2001 by Tang et al.[1] Interestingly, AIE, in which molecules of non-emissive in solution are induced to emit by aggregate formation, is exactly opposite to the aggregation-caused quenching (ACQ) effect. The unusual fluorescence behavior of AIE-active molecule has been successfully utilized to design sensitive and selective bio/chemosensors, particularly as bioprobes.[2-13] Typical AIE molecules, such as water-soluble tetraphenylethylene (TPE) derivatives[9,12] and 9,10-distyrylanthracene (DSA) derivatives,[10,11] have been used as fluorescent turn-on bioprobes for DNA detection. However, the binding modes between AIE-active molecules and *ds*DNA are virtually unexplored. The study of the binding modes of AIE-active molecules to nucleic acid will shed light on a deeper understanding of the mechanism of molecular interactions and facilitate the designing/preparation of new AIE-active bioprobes.

The binding mode between DNA and small molecules can be classified into different types. Besides covalent binding, small molecules can interact selectively with DNA by intercalation, groove binding or electrostatic interaction. Small differences in the molecular structure may greatly affect the binding modes, and thus the stability of the DNA-molecule complexes.[14-17] Classical techniques, such as UV–visible spectroscopy, fluorescence spectroscopy, cyclic voltammetry and CD spectroscopy, have been used to study the interactions between small molecules and DNA.[18] Among these techniques, CD spectroscopy is a simple and useful technique to provide important information about conformational properties of DNA and is usually used to investigate the binding modes of ligand-DNA interaction.[19-22] Besides, the single molecule techniques such as optical tweezers, AFM-based single molecule force spectroscopy (SMFS) and magnetic tweezers have been used to reveal structural and mechanical properties of synthetic and biopolymers.[23-33] The mechanical experiments with individual *ds*DNA molecules have provided new and direct insight into the structure and function of DNA.[34-36] AFM-based SMFS studies on *ds*DNA reveal the complex conformational changes in its double-helix secondary structures during stretching. It has been reported that under an external force of 65-70 pN the *ds*DNA undergoes a highly cooperative overstretching transition observed as a plateau in the force-extension profile.[36,37] A recent study indicates that the cooperativity of the overstretching transition strongly depends on the base stacking in the DNA double helix.[38] *ds*DNA is partially melted into *ss*DNA during the overstretching transition (*i.e.*, the stretched *ds*DNA exists as a mixture of the *ds*DNA segments and molten *ss*DNA segments) at the mechanical force of about 65 pN.[28,39]

It has been shown that different binding modes of small molecules to *ds*DNA can cause different perturbations in base stacking,[40-43] and the binding modes may be discriminated by the respective force-extension curves of *ds*DNA. For example, intercalators usually have the planar aromatic cores and insert between adjacent stacked bases,[44] this intercalation can cause an increase in contour length and decrease in persistence length of *ds*DNA (note: all of the terms of 'contour length' mentioned in the current paper indicate the length of

double stranded DNA, unless stated otherwise). Groove binders possessing net positive charges are likely to interact with DNA via an electrostatic interaction assisted by hydrogen bonds and van der Waals interactions.[23,45] The minor groove binders cause little change in contour length of *ds*DNA and an increase in persistence length in the low force region and a decrease in persistence length in the high force region. Major groove binders show no effect on the contour length and a decrease in persistence length.[43]

Although the overstretching behavior of DNA-ligand complex has been used to study the binding modes of model DNA-binding ligand (such as the typical intercalators, minor groove binders) to *ds*DNA, however, the binding modes between AIE-active molecules and *ds*DNA are virtually unexplored. In this study, we used the SMFS (as shown in Fig. 1A) and CD spectroscopy to study the interactions between *ds*DNA and four AIE-active molecules[9,11] (the structure is illustrated in Fig. 1B). The effects of molecular structure, concentration of AIE-active molecules, and ionic strength of buffer solutions on the nanomechanical properties of *ds*DNA were investigated. Different binding modes of these AIE molecules to *ds*DNA have been identified. In addition, effective ways for the control of binding strength between AIE-active molecule and *ds*DNA have been discussed.

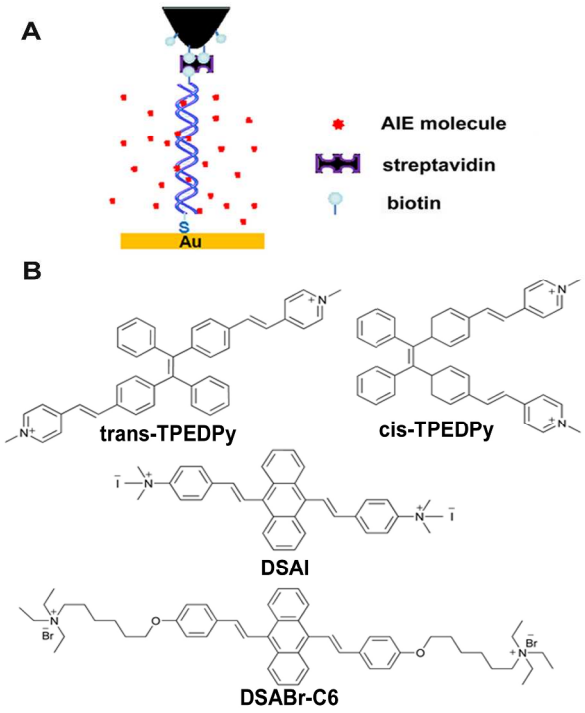

Fig. 1 (A) Schematic drawing of the stretching experiment. (B) Chemical structure of the AIE-active molecules used in the experiment.

Experimental

Sample preparation

High-purity deionized water (>18 MΩ•cm), produced from a Millipore system, was used for the preparation of all experimental buffers. The stock solution of small molecule (2×10^{-4} M) was prepared by dissolving an appropriate amount of small molecule in Tris-KCl-100 (10 mM tris-HCl, 100 mM KCl, pH 7.2) buffer solution. Experiments were carried out in aqueous Tris-KCl-100 buffer unless stated otherwise. For stretching experiments on small molecule-DNA complexes, the same concentration of small molecule as used for the formation of the complex was introduced into the buffer. For all experiments, dual-labeled linear DNA fragments (2000 bps) were obtained using PCR amplification with pCERoriD plasmid as a template.[46] HPLC-pure primers, 5'-biotin-CGCCACATAGCAGAACTT-3' and 5'-thiol-GCACCGCCTACATACCTC-3', were purchased from Sangon Biotech (Shanghai, China) to perform all these preparations. The PCR products were purified by using EasyPure PCR Purification Kit (TransGen Biotech, Beijing) and the concentration of DNA was quantified by using Helios UV-Visible spectrophotometer (Thermo Electronics) at 260 nm. Depending on the substrate size, 50-100 µL of the purified 5'-thiolated and 3'-biotin-labeled linear *ds*DNA (5 µg/mL) was absorbed from its solution onto a clean gold surface for 2 h, followed by immersing in 6-Mercapto-1-hexanol (MCH, from Sigma) solution (2.0 mM) for 30 min in order to desorb the DNA, which was immobilized on the surface by physisorption.[28] In doing this, the *ds*DNA was immobilized covalently to a gold surface via its thiolated end, leaving the biotin end exposed for picking up by AFM tip. And then the sample surface was rinsed with AIE-molecule containing buffer (0.5 µM, 2.0 µM or 4.0 µM) and the surface was finally incubated with 100 µL of respective small-molecule containing buffer for 30 min before the SMFS experiment.

Single molecule force spectroscopy

The force spectroscopy experiments were carried out on a ForceRobot (JPK instrument AG, Berlin, Germany) by using streptavidin (Promega) functionalized Si_3N_4 AFM tips (Bruker, Germany) as described before.[47,48] The spring constants of the employed AFM cantilevers were calibrated by the thermal noise method.[49,50] The measured values with different cantilevers ranged from 20 pN/nm to 25 pN/nm. During the stretching experiment, the streptavidin-coated AFM tip captures the biotin-labeled end of a single DNA molecule and travelled at a velocity of 1.0 µm/s for all the stretching-relaxation experiments.[47] Upon the addition of small molecules to the experimental buffer alterations in the extensibility of *ds*DNA were then investigated.

Circular dichroism

CD spectra were recorded using a MOS-450 spectrometer (Bio-Logic, France). The CD spectra of *ds*DNA in buffers with various ionic strengths and different concentrations (0-100 µM) of small molecules were measured using a 0.5 mm path length quartz cell in the 220–600 nm wavelength region at room temperature. The ratios were molar ratios of *ds*DNA (in base pairs) to small molecules. It need to be pointed that the solubility of small molecules was relatively low at room temperature, so the maximum ratio of small molecule to DNA was 1:3.8 in this experiment. The bandwidth was 1 nm, and the response time was 5 s.

Results and Discussion

Single molecule force spectroscopy

Effect of the concentration of small molecule on *ds*DNA conformation. Fig. 2 shows the typical force-extension curves of *ds*DNA in the presence of different concentrations of small molecules. Each stretching curve in the figure represents the typical curve obtained under corresponding condition, and more curves can be found in Fig. S1†. To quantify the change of contour and persistence length of *ds*DNA, we used the worm-like chain (WLC) model[43] to fit the low force region (0-40 pN) of each force-extension curve. Then statistical analysis was performed on the data to produce

the most probable value of contour/persistence length under each condition. As can be seen from Fig. 2 (as well as Fig. S2†, S3† and Table S1†), fits of the WLC model to stretching curves of *ds*DNA in the presence of three different AIE molecules show an increase in contour length and a decrease in persistence length as compared with that of pure *ds*DNA. With the increase of small molecules concentration the overstretching plateau of DNA gets shortened and the cooperativity of the overstretching transition gets decreased.

The DNA stretching curves obtained in the presence of those AIE molecules show great similarity to the curves observed in the presence of typical intercalators.[23,41,43,51-55] However, there are also some differences among stretching curves obtained on those three types of small molecule-DNA complexes. Firstly, upon the increase of small molecule concentration, the increased level/extents of contour length is different and the order is DSAI > *cis*-TPEDPy > *trans*-TPEDPy, see Table S1†. Secondly, the sensitivity of the change of DNA conformation to small molecule concentration is different. In the presence of low concentration of DSAI (0.5 μM), the stretching curves of DNA have notably changed as compared with that of pure *ds*DNA. The contour length of DNA molecule gets increased by 68.1 nm (from 461.1 nm to 529.3 nm), and overstretching transition plateau in the former case becomes shorter and tilted, which indicate that the content of helical structure gets decreased and the overstretching transition becomes less cooperative. In the presence of low concentration of *cis*-TPEDPy, the contour length change (24 nm) of DNA is much smaller than that in presence of DSAI. However, the presence of *cis*-TPEDPy caused the increase of mechanical stability and the decrease of the cooperativity of the DNA overstretching transition, which exhibits the character of groove binding. The presence of low concentration of *trans*-TPEDPy shows similar effect on the contour length of DNA as that of *cis*-TPEDPy but show no obvious effect on the stability of *ds*DNA. From the molecular structure (Fig. 1B) we can see that DSAI has a planar aromatic ring of anthracene. So the big increase of the contour length of DNA-DSAI complex as compared with that of pure DNA indicates that DSAI probably intercalates into adjacent DNA base pairs. However, owing to the steric hindrance of hydrophobic alkyl chains, DSABr-C6 is unable to intercalate into *ds*DNA and the main interaction of DSABr-C6 with DNA is electrostatic binding. Thus DSABr-C6 has almost no effect on the stretching curves of DNA even at very high concentration (see Fig. S4†). Both *cis*-TPEDPy and *trans*-TPEDPy have propeller-like shape thereby have more freedom to rotate. As a result, the intercalation between *cis*-/*trans*-TPEDPy and DNA are relatively weak and more complicated.

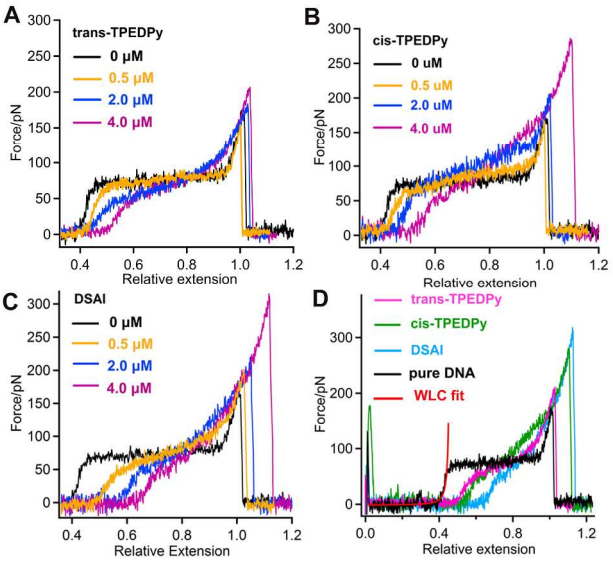

Fig. 2 Typical stretching curves of DNA molecules in the presence of different concentrations of small molecules (A) *trans*-TPEDPy, (B) *cis*-TPEDPy (C) DSAI in Tris-KCl-100 buffer. (D) A comparison of the stretching curves obtained in the Tris-KCl-100 aqueous solutions in the presence of 4.0 μM of *trans*-TPEDPy (pink), *cis*-TPEDPy (green), DSAI (blue). The stretching speed was 1.0 μm/s. The red curve shows a fit of WLC model to a DNA stretching curve.

Furthermore, we compared the force-extension curves of *ds*DNA in the presence of *trans*-TPEDPy, *cis*-TPEDPy and DSAI at a concentrations of 4.0 μM in Tris-KCl-100 aqueous solution, as shown in Fig. 2D. The result shows that apart from the difference in the contour length increment (DSAI > *cis*-TPEDPy > *trans*-TPEDPy), the binding of three small molecules has caused the reduction of the persistence length of *ds*DNA. DNA complexed with *cis*-TPEDPy exhibits a persistence length of 27.9 nm, whereas the persistence length of DNA-DSAI complex (40.2 nm) is close to that of *trans*-TPEDPy (42.7 nm). These results demonstrate that the binding of *trans*-TPEDPy to DNA exhibit intercalation effect, although the intercalation is weaker than other two small molecules. In particular, the differences of force-extension curves of *ds*DNA complexed with *cis*-TPEDPy and *trans*-TPEDPy suggest that these two isomers have markedly different effect on the conformation of DNA. A simple explanation for this phenomenon is that the intercalation moiety is different and the ability for stabilizing of DNA is different.

Effects of ionic strength on DNA-AIE molecule interactions. Considering the fact that all of the AIE molecules shown in Fig. 1B have positive charges, while the phosphate backbone of DNA show negative charges at neutral pH, electrostatic interactions may thus play important roles on these small molecule-DNA interactions. We then investigated the effect of ionic strength on the binding by stretching the small molecule-DNA complexes in aqueous solutions with various concentrations of salt while keeping the concentration of AIE molecule constant (0.5 μM).

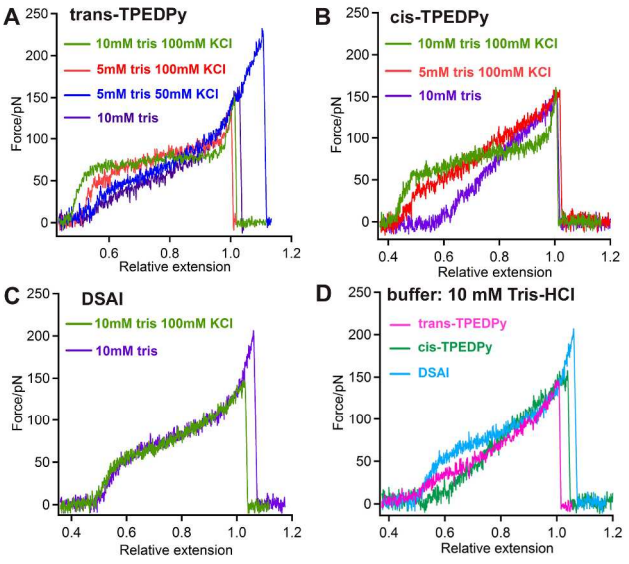

Fig. 3 Effects of ionic strength on the stretching curves of DNA obtained in the presence of 0.5 μM of (A) *trans*-TPEDPy, (B) *cis*-TPEDPy, (C) DSAI. (D) The comparison of the DNA stretching curves obtained at the low ionic strength of 10 mM Tris-HCl, pH 7.2.

In the presence of TPEDPy, the decrease of ionic strength causes

the increase of contour length and the decrease of persistence length of *ds*DNA greatly as shown in Fig. 3A and 3B (as well as in Fig. S5†, S6† and Table S2†). In addition, at a low ionic strength of 10 mM Tris-HCl, the overstretching transition of DNA has lost its cooperativity and the distinct plateau can no longer be observed. However, the decrease of ionic strength shows no obvious effects on the force-extension curves of DNA-DSAI complex, and only causes a slight increase of the contour length as well as a slight decrease of persistence length of DNA, as shown in Fig. 3C, Fig. S5†, S6† and Table S2†. This means that the interaction of DNA with DSAI is less sensitive to ionic strength and the main binding mode between DNA and DSAI is intercalation. The comparison of stretching curves of DNA complexed with DSAI, *cis*-TPEDPy and *trans*-TPEDPy at low ionic strength are shown in Fig. 3D. The results indicate that the interactions between *cis*-TPEDPy/*trans*-TPEDPy and DNA are sensitive to ionic strength and the interactions can be enhanced greatly with the decrease of ionic strength. Besides, ionic strength has a greater influence on the interactions between *cis*-TPEDPy and DNA compared with the case of *trans*-TPEDPy. The electrostatic interactions between the positively charged groups of the TPEDPy and the negatively charged phosphate DNA backbone have an important effect on the binding strength of TPEDPy with DNA. According to the fact that in the presence of TPEDPy (especially in the low salt solution), the overstretching transition plateau of *ds*DNA gets disappeared, we speculate that the possible binding modes of *cis*-/*trans*-TPEDPy to DNA are electrostatic interaction assisted intercalation.

The dissociation of AIE molecules from *ds*DNA. To get a deeper insight into the interactions between AIE-active molecules and DNA, we also investigated the dissociation process of those small molecules from DNA. The small molecule-DNA complexes were rinsed with a buffer containing no small molecules, and then incubated the DNA in this buffer for 30 min before the SMFS experiment. And then we recorded the stretching curves at different time intervals, and the data are shown in Fig. 4. During the experiments, two different types of salt concentrations (10 mM Tris-HCl, 100 mM KCl and 5 mM Tris-HCl, 50 mM KCl) were used to study the changes of force-extension curves of DNA over time, respectively. Our results show that in aqueous solutions of 10 mM Tris-HCl 100 mM KCl (high ionic strength) the force-extension curves obtained on DNA-TPEDPy complexes become indistinguishable to that of pure DNA within 30 min, as shown in Fig. 4A and 4B and Fig. S7†. In contrast, the force-extension curve of DNA-DSAI complexes was still distinctly different from that of pure DNA even after 14 h of incubation, as shown in Fig. 4C. This indicates that compared with DSAI it is easier for TPEDPy to get dissociated from the dsDNA.

According to the results shown above, we know that ionic strength has a great influence on the formation of TPEDPy-DNA complexes. To see such an effect on the reverse process (*i.e.*, the dissociation of the complexes), we compared the dissociation rate at the low ionic strength of 5 mM Tris-HCl 50 mM KCl (see Fig. 4D and 4E). Interestingly, the dissociation of *trans*-TPEDPy from DNA was faster than *cis*-TPEDPy under this condition. However, this difference was not evident at high ionic strength, as shown in Fig. 4A and 4B. This result indicates that the dissociation of TPEDPy from DNA depended strongly on the ionic strength which is consistent with the results on the binding process.

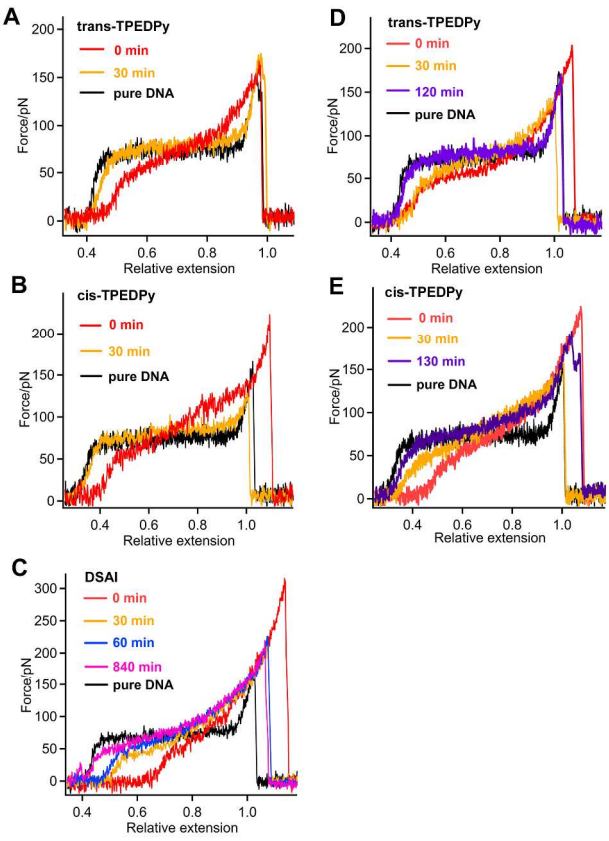

Fig. 4 Typical force-extension curves of DNA-small molecule complexes in AIE-molecule free buffer solution of (A-C) high (10 mM Tris-HCl, 100 mM KCl) and (D, E) low (5 mM Tris-HCl, 50 mM KCl) ionic strength. The complexes were formed in 2.0 μM AIE molecules (red traces), followed by washing and immersing with a buffer containing no small molecules for a certain time before the stretching.

Circular dichroism study

In order to further confirm the interaction modes of the above-mentioned molecules with DNA, we investigated the conformational changes of DNA in the absence and presence of small molecules by CD spectroscopy. Generally, the CD spectrum of B-form *ds*DNA exhibits one positive band at 275 nm due to the base stacking and one negative band at 245 nm due to the right-handed helicity.[56] And different binding modes of small molecules to DNA are known to cause different perturbations in base stacking and may therefore be discriminated by the changes of CD signals. Fig. 5A shows that with the increase of DSAI concentration, the intensity of the positive band at 275 nm increases remarkably while there is only a little change for the negative band at 245 nm, which indicates that DSAI mainly intercalates into DNA base pairs enhancing the base stacking and induces conformational change of DNA.[14,56] However, in the presence of DSABr-C6, the CD spectra of DNA show almost no change at 275 nm (see Fig. 5B), which indicates that intercalative interactions do not exist between DSABr-C6 and DNA. This finding is consistent with the SMFS results.

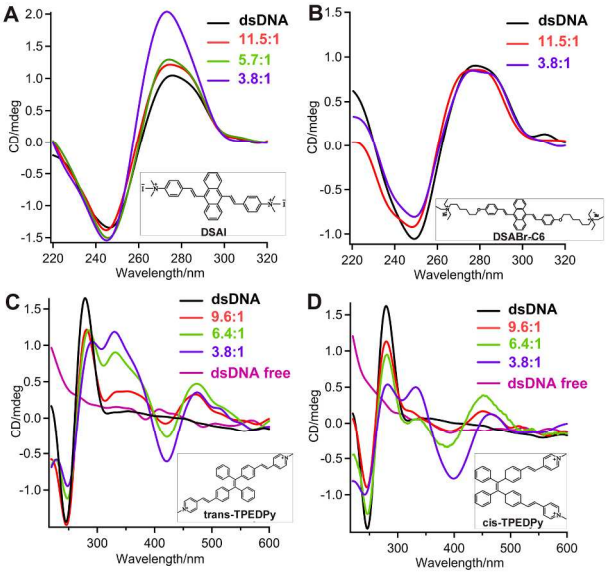

Fig. 5 CD spectra of *ds*DNA in the presence of various concentrations of (A) DSAI, (B) DSABr-C6, (C) *trans*-TPEDPy, (D) *cis*-TPEDPy, in Tris-KCl-100 buffer solution. The ratio is *ds*DNA (base pairs) molar concentration to small molecules.

The CD spectra of DNA in the presence of TPEDPy are more complicated than that of in the presence of DSAI (see Fig. 5C and 5D). With the addition of TPEDPy, the intensities of the positive band at 275 nm and negative band at 245 nm decreased remarkably, which indicates that the TPEDPy-binding induces certain conformational changes of *ds*DNA. Moreover, in contrast to *cis*-TPEDPy, the band at 275 nm is shifted of about 11 nm toward a longer wavelength when the ratio of *trans*-TPEDPy to DNA reaches 1:3.8. This may be attributed to the fact that *trans*-TPEDPy disrupt the base stacking of *ds*DNA and induce a partial B- to C-DNA conformational change of the secondary structure,[57,58] in which the minor groove becomes deeper and narrower and the major groove becomes shallower and wider. Besides, the magnitude of the decrease of CD intensity at 275 nm follows the order of *cis*-TPEDPy > *trans*-TPEDPy, which indicates that cis-TPEDPy possesses higher DNA-binding affinity than *trans*-TPEDPy does. These phenomena are consistent with the results obtained by SMFS.

Interestingly, TPEDPy is achiral and free to rotate having no intrinsic CD signal in the solution. However, upon interacting with DNA, the orientation of TPEDPy is restricted. Thus it exhibits an induced CD (ICD) signal in the 300-600 nm region through the coupling of electric transition moments of the TPEDPy and the DNA bases.[19] The ICD spectra of *cis*-TPEDPy consists of two positive band at 330 nm and 450 nm, and a negative band at 400 nm; while the positive bands of *trans*-TPEDPy appear at 330 nm and 475 nm, and the negative band was seen at 420 nm. The positive band at around 330 nm and the negative band at around 400 nm are significantly enhanced as the concentration of TPEDPy is increased, while the band at around 450 nm is not sensitive to the concentrations of TPEDPy. These complex signals of ICD may be attributed to the greater number of possible orientations permitted by the width of the major groove.[59] Therefore we speculate that the possible pathway for TPEDPy-binding is through the intercalation into DNA from the major groove direction. In addition, we also obtained the CD spectra of *ds*DNA in the presence of *cis*-TPEDPy and *trans*-TPEDPy at various ionic strengths (Fig. S8†). The results show that the reduction of ionic strength causes the further decrease of 275 nm CD intensity, which support the SMFS results that TPEDPy-DNA interactions are sensitive to ionic strength.

Conclusions

By using AFM-based SMFS together with CD spectroscopy, we have systematically investigated the interactions between four AIE-active molecules and DNA. SMFS results indicate that DSAI and TPEDPy molecules all show intercalative interactions with DNA in the buffer of Tris-KCl-100 and the relative intercalation strengths varied in the order DSAI > *cis*-TPEDPy > *trans*-TPEDPy. It is also found that, *trans*-TPEDPy and *cis*-TPEDPy are sensitive to ionic strength, and low ionic strength can enhance greatly the intercalative interactions with DNA. The intercalation of DSAI to DNA is less sensitive to ionic strength. DSABr-C6 is difficult to intercalate into *ds*DNA because of steric hindrance of hydrophobic alkyl chains. Moreover CD spectroscopy experiment demonstrated that the interactions between TPEDPy and DNA exhibit both intercalative binding and major groove binding. Putting all the data together, we can suppose the possible binding modes of *cis*-TPEDPy and *trans*-TPEDPy with DNA as follows: *cis*-TPEDPy grab the negatively charged phosphate backbones of *ds*DNA via its two positive hands (*i.e.*, cations of pyridinium), especially in solution with low ionic strength, as a result the freedom of the two phenyl groups of tetraphenylethylene are restricted facilitating the intercalation of phenyl groups into DNA base pairs, while *trans*-TPEDPy can only intercalate into DNA base pairs via a phenyl group. Further investigations on the direct quantitative measurement of interactions between AIE molecules and DNA are underway.

Acknowledgements

This work was supported by the National Basic Research Program (2013CB834503, 2013CB834704), the National Science Foundation of China (Grant Nos. 21221063, 91127031) and the Program for New Century Excellent Talents in University (NCET-11-0205). The pCERoriD plasmid was a gift from Prof. Panos Soultanas (Nottingham University, UK).

Notes and references

[a] State Key Laboratory of Supramolecular Structure and Materials, College of Chemistry, Jilin University, Changchun, 130012, P. R. China; Tel: +86-431-85159203; E-mail: zhangwk@jlu.edu.cn

[b] MOE Key Laboratory of Macromolecule Synthesis and Functionalization, Department of Polymer Science and Engineering, Zhejiang University, Hangzhou, 310027, China.

‡ These authors contributed equally to this work, and should be looked on as co-first author.

† Electronic Supplementary Information (ESI) available: More typical force-extension curves of *ds*DNA in the presence of different concentration of AIE-active molecules. Effects of ionic strength on the CD spectra of *ds*DNA-TPEDPy complexes.

1 J. Luo, Z. Xie, J. W. Y. Lam, L. Cheng, H. Chen, C. Qiu, H. S. Kwok, X. Zhan, Y. Liu, D. Zhu and B. Z. Tang, *Chem. Commun.*, 2001, 1740-1741.

2 H. Tong, Y. Hong, Y. Q. Dong, M. Häussler, Z. Li, J. W. Y. Lam, Y. P. Dong, H. H.-Y. Sung, I. D. Williams and B. Z. Tang, *J. Phys. Chem. B,* 2007, **111**, 11817-11823.

3 M. Wang, D. Q. Zhang, G. X. Zhang, Y. L. Tang, S. Wang and D. B. Zhu, *Anal. Chem.*, 2008, **80**, 6443-6448.

4 Q. Chen, N. Bian, C. Cao, X. L. Qiu, A. D. Qi and B. H. Han, *Chem. Commun.,* 2010, **46**, 4067-4069.
5 Y. Liu, C. M. Deng, L. Tang, A. J. Qin, R. R. Hu, J. Z. Sun and B. Z. Tang, *J. Am. Chem. Soc.,* 2011, **133**, 660-663.
6 K. Li and B. Liu, *Polym. Chem*., 2010, **1**, 252-259.
7 H. B. Shi, R. T. K. Kwok, J. Z. Liu, B. G. Xing, B. Z. Tang and B. Liu, *J. Am. Chem. Soc.*, 2012, **134**, 17972-17981.
8 A. Qin, J. W. Y. Lam and B. Z. Tang, *Prog. Polym. Sci*., 2012, **37**, 182-209.
9 J. K. Jin, X. J. Chen, Y. Liu, A. J. Qin, J. Z. Sun and B. Z. Tang, *Acta. Polym. Sin.*, 2011, **9**, 1079-1085.
10 H. G. Lu, B. Xu, Y. J. Dong, F. P. Chen, Y. W. Li, Z. F. Li, J. T. He, H. Li and W. J. Tian, *Langmuir*, 2010, **26**, 6838-6844.
11 X. Li, K. Ma, S. J. Zhu, S. Y. Yao, Z. Y. Liu, B. Xu, B. Yang and W. J. Tian, *Anal. Chem.*, 2014, **86**, 298-303.
12 L. Xu, Z. C. Zhu, X. Zhou, J. G. Qin and C. L. Yang, *Chem. Commun.*, 2014, **50**, 6494-6497.
13 L. Xu, Z. C. Zhu, D. Q. Wei, X. Zhou, J. G. Qin and C. L. Yang, *ACS Appl. Mater. Interfaces*, 2014, **6**, 18344-18351.
14 T. Jia, J. Xiang, J. Wang, P. Guo and J. P. Yu, *Org. Biomol. Chem*., 2013, **11**, 5512-5520.
15 A. Gluszynska, K. Bajor, I. Czerwinska, D. Kalet and B. Juskowiak, *Tetrahedron Lett*., 2010, **51**, 5415-5418.
16 S. Catoen-Chackal, M. Facompré, R. Houssin, N. Pommery, J.-F. Goossens, P. Colson, C. Bailly and J.-P. Hénichart, *J. Med. Chem.*, 2004, **47**, 3665-3673.
17 A. Manna and S. Chakravorti, *J. Phys. Chem. B*, 2012, **116**, 5226-5233.
18 M. Sirajuddin, S. Ali and A. Badshah, *J. Photoch. Photobio. B*, 2013, **124**, 1-19.
19 N. C. Garbett, P. A. Ragazzon and J. B. Chaires, *Nat. Protoc.*, 2007, **2**, 3166-3172.
20 M. Saminathan, T. Antony, A. Shirahata, L. H. Sigal, T. Thomas and T. J. Thomas, *Biochemistry*, 1999, **38**, 3821-3830.
21 H. Ihmels, K. Faulhaber, D. Vedaldi, F. Dall'Acqua, G. Viola, *Photochem. Photobiol.*, 2005, **81**, 1107-1115.
22 K. Bhadra, M. Maiti and G. S. Kumar, *Chem. Biol.*, 2008, **5**, 575-590.
23 R. Krautbauer, L. H. Pope, T. E. Schrader, S. Allen and H. E. Gaub, *FEBS Lett.,* 2002, **510**, 154-158.
24 D. Anselmetti, J. Fritz, B. Smith and X. Fernandez-Busquets, *Single Mol.*, 2000, **1**, 53-58.
25 R. Krautbauer, H. Clausen-Schaumann and H. E. Gaub, *Angew. Chem. Int. Ed.*, 2000, **39**, 3912-3915.
26 A. Goel, M. D. Frank-Kamenetskii, T. Ellenberger and D. Herschbach, *Proc. Natl. Acad. Sci. U.S.A.*, 2001, **98**, 8485-8489.
27 D. E. Smith, S. J. Tans, S. B. Smith, S. Grimes, D. L. Anderson and C. Bustamante, *Nature*, 2001, **413**, 748-752.
28 N. N. Liu, T. J. Bu, Y. Song, W. Zhang, J. J. Li, W. K. Zhang, J. C. Shen and H. B. Li, *Langmuir*, 2010, **26**, 9491-9496.
29 Y. G. Pan, F. Wang, Y. H. Liu, J. G. Jiang, Y.-G. Yang and H. D. Wang, *Nanoscale*, 2014, **6**, 13421-13424.
30 Y. Bao, H.-J. Qian, Z.-Y. Lu and S. X. Cui, *Nanoscale*, 2014, **6**, 13421-13424.
31 B. Cheng, S. G. Wu, S. X. Liu, P. Rodriguez-Aliaga, J. Yu and S. X. Cui, *Nanoscale*, 2015, **7**, 2970-2977.
32 J. M. Hamill, K. Wang and B. Q. Xu, *Nanoscale*, 2014, **6**, 5657-5661.
33 C. Lv, X. Gao, W. Li, B. Xue, M. Qin, L. D. Burtnick, H. Zhou, Y. Cao, R. C. Robinson and W. Wang, *Nat Commun*, 2014, **5**, 4623.
34 C. Bustamante, S. B. Smith, J. Liphardt and D. Smith, *Curr. Opin. Struct. Biol.*, 2000, **10**, 279-285.
35 T. R. Strick, J.-F. Allemand, D. Bensimon and V. Croquette, *Annu. Rev. Biophys. Biomol. Struct.*, 2000, **29**, 523-543.
36 H. Clausen-Schaumann, M. Rief, C. Tolksdorf and H. E. Gaub, *Biophys. J.*, 2000, **78**, 1997-2007.
37 M. Rief, H. Clausen-Schaumann and H. E. Gaub, *Nat. Struct. Biol*., 1999, **6**, 346-349.
38 H. J. Zhou, Y. Zhang and Z. C. Ou-Yang, *Phys. Rev. Lett*., 1999, **82**, 4560-4563.
39 J. R. Wenner, M. C. Williams, I. Rouzina and V. A. Bloomfield, *Biophys. J.*, 2002, **82**, 3160-3169.
40 M. C. Williams, I. Rouzina, J. R. Wenner, R. J. Gorelick, K. Musier-Forsyth and V. A. Bloomfield, *Proc. Natl. Acad. Sci. U.S.A.*, 2001, **98**, 6121-6126.
41 I. D. Vladescu, M. J. McCauley, M. E. Nunez, I. Rouzina and M. C. Williams, *Nat. Methods*, 2007, **4**, 517-522.
42 T. Paramanathan, I. Vladescu, M. J. McCauley, I. Rouzina and M. C. Williams, *Nucleic. Acids. Res*., 2012, **40**, 4925-4932.
43 K. R. Chaurasiya, T. Paramanathan, M. J. McCauley and M. C. Williams, *Phys. Life. Rev.*, 2010, **7**, 299-341.
44 S. Neidle and Z. Abraham, *CRC. Cri. Rev. Biochem.*, 1984, **17**, 73-121.
45 R. Eckel, R. Ros, A. Ros, S. D. Wilking, N. Sewald and D. Anselmetti, *Biophys. J.,* 2003, **85**, 1968-1973.
46 W. K. Zhang, M. S. Dillingham, C. D. Thomas, S. Allen, C. J. Roberts and P. Soultanas, *J. Mol. Biol.*, 2007, **371**, 336-348.
47 W. K. Zhang, C. Machon, A. Orta, N. Phillips, C. J. Roberts, S. Allen and P. Soultanas, *J. Mol. Biol.*, 2008, **377**, 706-714.
48 W. K. Zhang, R. Barbagallo, C. Madden, C. J. Roberts, A. Woolford and S. Allen, *Nanotechnology*, 2005, **16**, 2325-2333.
49 J. L. Hutter and J. Bechhoefer, *Rev. Sci. Instrum.*, 1993, **64**, 1868-1873.
50 H.-J. Butt and M. Jaschke, *Nanotechnology*, 1995, **6**, 1-7.
51 D. H. Paik and T. T. Perkins, *Angew. Chem. Int. Ed.*, 2012, **51**, 1811-1815.
52 A. Sischka, K. Toensing, R. Eckel, S. D. Wilking, N. Sewald, R. Ros and D. Anselmetti, *Biophys. J.*, 2005, **88**, 404-411.
53 A. Mihailovic, I. Vladescu, M. McCauley, E. Ly, M. C. Williams, E. M. Spain and M. E. Nunez, *Langmuir*, 2006, **22**, 4699-4709.
54 M. J. McCauley and M. C. Williams, *Biopolymers*, 2006, **85**, 154-168.
55 R. Krautbauer, S. Fischerländer, S. Allen and H. E. Gaub, *Single Mol.,* 2002, **3**, 97-103.
56 J. Wang and X. Y. Yang, *Spectrochim. Acta. A*, 2009, **74**, 421-426.
57 Z. H. Xu, F. J. Chen, P. X. Xi, X. H. Liu and Z. Z. Zeng, *J. Photoch. Photobio. A*, 2008, **196**, 77-83.
58 C. S. Braun, G. S. Jas, S. Choosakoonkriang, G. S. Koe, J. G. Smith and R. Middaugh, *Biophys. J.*, 2003, **84**, 1114-1123.
59 R. Lying, A. Rodger and B. Nordén, *Biopolymers*, 1991, **31**, 1709-1720.

